Discrete Geometric Approach for the Three-Dimensional Schrödinger Problem and Comparison With Finite Elements

Ruben Specogna and Francesco Trevisan

Università di Udine, Dipartimento di Ingegneria Elettrica, Gestionale e Meccanica, Udine 33100, Italy

The numerical modeling of nanoscale electron devices needs the development of accurate and efficient numerical methods, in particular, for the numerical solution of the Schrödinger problem. If FEMs allow an accurate geometric representation of the device, they lead to a discrete counterpart of Schrödinger problem in terms of a computationally heavy generalized eigenvalue problem. Exploiting the geometric structure behind the Schrödinger problem, we will construct a numerically efficient discrete counterpart of it, yielding to a standard eigenvalue problem. We will also show how the two approaches are only partially akin to each other even when lumping is applied.

Index Terms—**FEM, nanoelectronics, Schrodinger equation, semiconductor device modeling.**

I. Introduction

MODERN microelectronics and optoelectronics use semiconductor materials structured at truly nanometric dimensions [1]. As an example, the silicon technology is now approaching the physical limits for the traditional bulk MOS devices, since the carrier transport is confined in very thin semiconductor layers; moreover, new device architectures like silicon nanowire FETs and fin-shaped FETs (FinFETs) are under investigation as valid alternatives [2].

The modeling of such nanoscale electron devices is based on multiphysics simulations, where transport equation or electrostatics are coupled with the Schrödinger problem [3] whose numerical solution still remains the key bottleneck of the simulation. For this reason, we focus on the development of accurate and efficient numerical methods for the solution of the Schrödinger problem in the effective mass approximation [4].

In this framework, one of the purposes of this paper is to show how the geometric structure behind the Schrödinger problem, formulated in arbitrarily 3-D-shaped domains, leads to a numerically efficient discrete counterpart consisting of a standard eigenvalue problem. Such a result follows from the so-called discrete geometric approach (DGA) [5]. On the contrary, finite elements (FE) discretization yields to a computationally heavy generalized eigenvalue problem.

We will also show how the discrete counterpart of the Schrödinger problem, deduced from DGA, and that from FE are only partially related by a lumping technique. Finally, a numerical comparison between the two discrete counterparts is also given in terms of convergence with mesh refinement and accuracy.

II. Schrödinger Equation Reformulated

We focus on a 3-D spatial domain D, individuated by the Cartesian components (x, y, z) of the position vector r (vectors and tensors are denoted in roman type) of a particle; the medium properties are described by a diagonal double tensor[1] $q(r)$ whose ijth Cartesian component, with $i, j = 1, \ldots, 3$, is

$$q_{ij}(r) = \frac{\hbar^2}{2m_i(r)}\delta_{ij} \tag{1}$$

where $\hbar$ is the reduced Plank constant and $m_i(r)$ is the effective mass coefficient of the particle, along the ith Cartesian axis; δ_{ij} is the Kronecker symbol. We also denote with λ the eigenvalue (or energy level) and with $\psi(r)$ the corresponding eigenfunction evaluated at a point r; $m_i(r)$ is here assumed independent of λ. Finally, $u(r)$ denotes the confinement potential energy term in D, considered known in this paper. Now, we introduce a pair of vector fields $a(r)$, $b(r)$ and a scalar field $\phi(r)$ in such a way that

$$-\text{grad}\,\psi(r) = a(r) \tag{2}$$

$$\text{div}\, b(r) = \phi(r) \tag{3}$$

and

$$q(r)a(r) = b(r) \tag{4}$$

$$(\lambda - u(r))\psi(r) = \phi(r) \tag{5}$$

hold simultaneously. Of course, boundary conditions on ∂D and interface conditions must be considered in addition to close the problem. It is apparent that (2), (4), (3), and (5) are equivalent to the standard time-independent Schrödinger problem [4]

$$-\text{div}\, q(r)\text{grad}\,\psi(r) = (\lambda - u(r))\,\psi(r). \tag{6}$$

III. Discrete Geometric Approach for the Schrödinger Problem

To compute a discrete geometric counterpart of the Schrödinger problem (2), (4), (3) and (5), we introduce in D a pair of interlocked cell complexes: the primal and the dual complexes, [6]; without losing generality, we will focus on a primal complex formed by a single tetrahedron. The geometric construction can be easily generalized to a primal complex of tetrahedra. The primal cell complex $\mathcal{K} = \{\mathcal{N},\ \mathcal{E},\ \mathcal{F},\ \mathcal{V}\}$, consists of nodes $n_i \in \mathcal{N}$, edges $e_j \in \mathcal{E}$, faces $f_h \in \mathcal{F}$ (triangles), and volumes $v_k \in \mathcal{V}$ (the tetrahedron), all endowed with an orientation; the cardinality of each set $\mathcal{N},\ \mathcal{E},\ \mathcal{F},\ \mathcal{V}$ is denoted by $N = 4$, $E = 6$, $F = 4$, and $V = 1$, respectively. From $\mathcal{K}$, we construct the barycentric dual complex $\tilde{\mathcal{K}} = \{\tilde{\mathcal{V}},\ \tilde{\mathcal{F}},\ \tilde{\mathcal{E}},\ \tilde{\mathcal{N}}\}$, here tailored within the tetrahedron [6,5] v_k. The geometrical elements, respectively,

Manuscript received June 23, 2013; revised August 11, 2013; accepted September 4, 2013. Date of current version February 21, 2014. Corresponding author: R. Specogna (e-mail: ruben.specogna@uniud.it).

Color versions of one or more of the figures in this paper are available online at http://ieeexplore.ieee.org.

Digital Object Identifier 10.1109/TMAG.2013.2281073

[1]The double tensor may be a general symmetric and positive definite matrix.

are: dual nodes $\tilde{n}_k \in \tilde{\mathcal{N}}$ being the center of mass of the primal volume v_k, dual edges $\tilde{e}_h \in \tilde{\mathcal{E}}$, dual faces $\tilde{f}_j \in \tilde{\mathcal{F}}$ and dual volumes $\tilde{v}_i \in \tilde{\mathcal{V}}$.

The topology of the complexes is accounted by means of standard incidence matrices: $\mathbf{G}$ of dimension $E \times N$ of incidence numbers G_{ji} between the orientations of (e_j, n_i), matrix $\mathbf{D}$ of dimension $V \times F$ of incidence numbers D_{kh} between the orientations of (v_k, f_h) and matrix $\tilde{\mathbf{D}} = -\mathbf{G}^T$ of dimension $N \times E$ of incidence numbers between the orientations of $(\tilde{v}_i, \tilde{f}_j)$.

We need to introduce integrals of the vectors a, b and of the scalars $\psi(r)$, $\phi(r)$ fields associated with the geometric elements of $\mathcal{K}$, $\tilde{\mathcal{K}}$ as follows. The array $\mathbf{\Psi}$ of dimension N, whose ith entry $\Psi_i = \psi(r_i)$ with $i = 1, \dots N$, is the value $\psi(r_i)$ assumes in the position r_i of the node n_i; Ψ_i is associated with primal nodes. The array $\mathbf{A}$ of dimension E whose jth entry is the circulation $A_j = \int_{e_j} a(r) \cdot dl$ of the vector $a(r)$ along a primal edge e_j, with $j = 1, \dots E$; it is associated with primal edges. The array $\mathbf{B}$ of dimension E whose jth entry is the flux $B_j = \int_{\tilde{f}_j} b(r) \cdot ds$ of the vector $b(r)$ across a dual face $\tilde{f}_j$ with $j = 1, \dots E$; it is associated with dual faces. The array $\mathbf{\Phi}$ of dimension N whose ith entry

$$\Phi_i = \int_{\tilde{v}_i} \phi(r) dv \tag{7}$$

is associated with a dual volume $\tilde{v}_i$, with $i = 1, \dots N$.

We can straightforwardly construct exact discrete counterparts of (2) and (3), respectively, in terms of the introduced arrays with respect to the cell complexes $\mathcal{K}$, $\tilde{\mathcal{K}}$, [6], [5]

$$-\mathbf{G}\mathbf{\Psi} = \mathbf{A} \tag{8}$$

$$-\mathbf{G}^T\mathbf{B} = \mathbf{\Phi} \tag{9}$$

and approximated discrete counterparts for (4) and (5)

$$\mathbf{M}\mathbf{A} = \mathbf{B} \tag{10}$$

$$\mathbf{N}\mathbf{\Psi} = \mathbf{\Phi} \tag{11}$$

where $\mathbf{M}$ and $\mathbf{N}$ are square matrices of dimension E and N, respectively, depending on the metric and media properties of the pair of cell complexes.

Substituting (8) and (10) in (9), a discrete counterpart of the problem (2), (3), (4) is expressed by the following problem:

$$\mathbf{S}\mathbf{\Psi} = \mathbf{\Phi} \tag{12}$$

where $\mathbf{S} = \mathbf{G}^T\mathbf{M}\mathbf{G}$ is the so called stiffness matrix.

Under the hypothesis of element-wise uniform vector fields $a(r)$, $b(r)$ in each v_k, we proved [5] that the entry S_{ij} of $\mathbf{S}$ for a primal complex made of a single tetrahedron v_k of volume $|v_k|$, can be expressed in a pure geometric way as

$$S_{ij} = \frac{1}{9|v_k|} D_{ki}\mathrm{f}_i \cdot q\, D_{kj}\mathrm{f}_j, \qquad i, j = 1, \dots 4 \tag{13}$$

where f_i is the vector having as amplitude the area of the face f_i, normal to the face and oriented in a congruent way as the orientation of the face. For a primal complex made of $V > 1$ tetrahedra, the matrix $\mathbf{S}$ can be obtained by assembling the contributions (13) from each tetrahedron v_k.

Using the result already proved in [7, eq. (6)], it can be easily seen that $S_{ij} = \int_{v_k} \mathrm{grad} w_i \cdot q\, \mathrm{grad} w_j\, dv$ holds, which is the stiffness matrix for the tetrahedron v_k in the case of Finite Elements with an affine representation of ψ in terms of the standard nodal affine base functions w_j for v_k, [8].

To compute matrix $\mathbf{N}$, we substitute (5) in (7), obtaining for a single tetrahedron v_k

$$\Phi_i = \int_{\tau_{ik}} \lambda \psi(r) dv - \int_{\tau_{ik}} u(r)\psi(r) dv \tag{14}$$

where $\tau_{ik} = \tilde{v}_i \cap v_k$ and $i = 1, \dots, N$. Then, we introduce a piecewise uniform base function $\bar{w}_i(r)$, attached to a primal node n_i, with $i = 1, \dots, N$, such that

$$\bar{w}_i(r) = \begin{cases} 1 & \text{if } r \in \tau_{ik} \\ 0 & \text{elsewhere} \end{cases} \tag{15}$$

holds. Base functions $\bar{w}_i(r)$ represent exactly a piecewise uniform scalar field $\bar{\psi}(r)$ in D as

$$\bar{\psi}(r) = \sum_{i=1}^{N} \bar{w}_i(r)\, \bar{\Psi}_i \tag{16}$$

where $\bar{\Psi}_i$ denotes the nodal value $\bar{\psi}(r)$ assumes at the node n_i.

Next, by substituting (16) in (14) for ψ, we obtain

$$\bar{\Phi}_i = \bar{\lambda}\, \frac{|v_k|}{4}\, \bar{\Psi}_i - \int_{\tau_{ik}} u(r) dv\, \bar{\Psi}_i \tag{17}$$

where, in the first addendum, we used the geometric identity $|v_k| = 4|\tau_{ik}|$. Assuming an affine distribution of the potential energy $u(r)$ in v_k $u(r) = \sum_{j=1}^{N} w_j(r)\, u_j$ for $r \in v_k$, the last integration in (17) over the hexahedron τ_{ik}, with little algebra, yields

$$U_i = \int_{\tau_{ik}} u(r) dv = \sum_{j=1}^{N} \frac{|v_k|}{4} \left(\frac{23}{144} + \frac{13}{36}\delta_{ij} \right) u_j \tag{18}$$

u_j being the value $u(r_{n_j})$ assumes at node n_j of v_k.

From (17), we deduce the entries of a constitutive matrix $\bar{\mathbf{N}}$, mapping $\bar{\mathbf{\Psi}}$ to $\bar{\mathbf{\Phi}}$ according to (11)

$$(\bar{\mathbf{N}})_{ij} = \bar{\lambda}\, \frac{|v_k|}{4}\delta_{ij} - U_i\delta_{ij} = \bar{\lambda}(\bar{\mathbf{T}})_{ij} - (\bar{\mathbf{U}})_{ij}, \tag{19}$$

partitioned as the sum of the pair of diagonal matrices $\bar{\mathbf{T}}$, $\bar{\mathbf{U}}$, respectively.

On a pair of interlocked cell complexes of V tetrahedra and N nodes, we assemble the global matrices $\mathbf{S}$, $\bar{\mathbf{N}} = \bar{\lambda}\bar{\mathbf{T}} - \bar{\mathbf{U}}$ from the local matrices (13), (19) deduced for the single tetrahedron v_k, respectively; substituting (11) in (12), we obtain a discrete counterpart of the Schrödinger problem based on a piecewise uniform approximation of ψ as

$$(\mathbf{S} + \bar{\mathbf{U}})\, \bar{\mathbf{\Psi}} = \bar{\lambda}\bar{\mathbf{T}}\, \bar{\mathbf{\Psi}} \tag{20}$$

where, the array $\bar{\mathbf{\Psi}}$, of dimension N, contains the nodal values of ψ and the square matrices $\mathbf{S}$, $\bar{\mathbf{U}}$, $\bar{\mathbf{T}}$ have dimension N; moreover, the entries of $\bar{\mathbf{U}}$ are deduced using an affine approximation of $u(r)$ in D and the metric of the dual complex. An important result of the geometric discretization approach is that $\bar{\mathbf{T}}$ is diagonal; thus (20) can be easily and efficiently transformed into a standard eigenvalue problem.

IV. FE Generalized Eigenvalue Problem and Lumping

According to the FE method [8] based on the affine approximations of $\psi(r)$ and $u(r)$ in terms of the affine nodal base functions w_j, the discrete counterpart of the Schrödinger problem yields the following generalized eigenvalue problem:

$$(\mathbf{S} + \mathbf{U}_{\mathrm{FE}})\, \mathbf{\Psi}_{\mathrm{FE}} = \lambda_{\mathrm{FE}} \mathbf{T}_{\mathrm{FE}}\, \mathbf{\Psi}_{\mathrm{FE}} \tag{21}$$

where the entries of $\mathbf{T}_{\mathrm{FE}}$ and $\mathbf{U}_{\mathrm{FE}}$ are written, respectively, as

$$(\mathbf{T}_{\mathrm{FE}})_{ij} = \int_D w_i w_j \, dv \tag{22}$$

$$(\mathbf{U}_{\mathrm{FE}})_{ij} = \int_D w_i w_j u \, dv \tag{23}$$

with $i, j = 1, \ldots, N$. In order to transform (21) into a standard eigenvalue problem, it is usual to apply the so called *lumping* technique [8], [9] to the matrix $\mathbf{T}_{\mathrm{FE}}$, obtaining

$$(\mathbf{S} + \mathbf{U}_{\mathrm{FE}})\, \mathbf{\Psi}_l = \lambda_l\, \mathbf{T}_l\, \mathbf{\Psi}_l \tag{24}$$

where the lumped matrix $\mathbf{T}_l$ is diagonal, with entries

$$(\mathbf{T}_l)_{ii} = \sum_{j=1}^{N} (\mathbf{T}_{\mathrm{FE}})_{ij} \tag{25}$$

for $i = 1, \ldots, N$. Moreover, between the eigenvalues of (21) and of (24) the following relations $\lambda \leq \lambda_{\mathrm{FE}}$ and $\lambda_l \leq \lambda_{\mathrm{FE}}$ hold [8]–[10], λ being the eigenvalue of (6).

We will now demonstrate the link between lumping applied to the FE matrix $\mathbf{T}_{\mathrm{FE}}$ and the matrix $\bar{\mathbf{T}}$ from discrete geometric approach.

Property 1: We have that $\mathbf{T}_l = \bar{\mathbf{T}}$ holds.

Remark 1: Even though the $\bar{\mathbf{U}}$ matrix obtained with DGA is diagonal, it is different with respect to the lumping of the corresponding $\mathbf{U}_{\mathrm{FE}}$ matrix obtained with FE. As a consequence, the results provided by DGA and by FE in term of eigenvalues and eigenvectors are in general different, even if lumping is applied on both $\mathbf{U}_{\mathrm{FE}}$ and $\mathbf{T}_{\mathrm{FE}}$ matrices.

Proof: Observing that for tetrahedron v_k

$$\int_{v_k} w_i w_j \, dv = (1 + \delta_{ij}) \frac{|v_k|}{20}, \qquad i, j = 1, \ldots, 4 \tag{26}$$

holds and that $D = \bigcup_{k=1}^{V} v_k$, we may rewrite (22) as

$$\int_D w_i w_j \, dv = \frac{1}{10} \sum_{k \in \mathcal{C}(n_i)} |v_k|, \qquad \text{if } i = j \tag{27}$$

$$\int_D w_i w_j \, dv = \frac{1}{20} \sum_{k \in \mathcal{C}(n_i, n_j)} |v_k|, \qquad \text{if } i \neq j \tag{28}$$

where we denoted with $C(n_i)$ the set of labels of the cluster of tetrahedra having n_i as common node and with $\mathcal{C}(n_i, n_j) = \mathcal{C}(e_m)$ the set of labels of the cluster of tetrahedra having the edge e_m, between the nodes n_i, n_j, in common, with $i, j = 1, \ldots, N$; of course, when the set $\mathcal{C}(n_i, n_j)$ is empty then the right hand side of (28) yields zero. Now, applying the lumping technique (25) and using (27), (28), we obtain

$$(\mathbf{T}_l)_{ii} = \sum_{j=1}^{\mathcal{N}} (\mathbf{T}_{\mathrm{FE}})_{ij} \tag{29}$$

$$= \frac{1}{10} \sum_{k \in \mathcal{C}(n_i)} |v_k| + \frac{1}{20} \sum_{j=1, j \neq i}^{N} \sum_{k \in \mathcal{C}(n_i, n_j)} |v_k| \tag{30}$$

$$= \frac{1}{10} \sum_{k \in \mathcal{C}(n_i)} |v_k| + \frac{3}{20} \sum_{k \in \mathcal{C}(n_i)} |v_k| = (\bar{\mathbf{T}})_{ii}, \tag{31}$$

where in the last summation of (30) the volume $|v_k|$ of each tetrahedron v_k is counted three times since there are always three edges drawn from a node n_i belonging to v_k; this yields the last addendum of (31) and from the definition of $(\bar{\mathbf{T}})_{ij}$ in (19) the thesis follows. ■

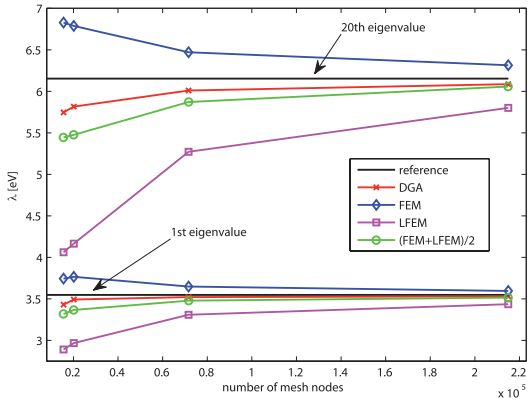

Fig. 1. Convergence with respect to mesh refinement of the first and 20th eigenvalues for the cube benchmark.

V. Numerical Results

The formulations have been integrated into the Geometric Approach to Maxwell's Equations (GAME) Fortran 90 code developed by the authors. The state-of-the-art FEAST [11] library has been employed to solve the generalized eigenvalue problems, whereas TRLan [12] is used for standard eigenvalue problems.

To validate the results produced by the described formulations and compare them, a particle in a box benchmark—which admits a pseudo analytical solution using pseudospectral methods [2]—has been analyzed. This benchmark consists of a cube of edge $d = 10$ nm in which the energy distribution $u(r) = x + y + z$ eV is assumed, where x, y, z range from 0 to 10 nm, and q is a homogeneous, anisotropic diagonal tensor $q = \mathrm{diag}(0.04159, 0.20053, 0.20053)$. In Fig. 1, the convergence with respect to mesh refinement of the first and 20th eigenvalues computed by DGA, finite elements (FEM) and lumped finite elements (LFEM) is compared. Obviously, the same mesh is used for all the considered methods. Moreover, the mean between FEM and LFEM is also considered, since it is claimed in some papers that the two formulations provide upper and lower bounds for eigenvalues [10]. The DGA exhibits superior accuracy with respect to FEM and LFEM techniques and this behavior holds for all eigenvalues, as Fig. 3 shows for the first 20.

As a more practical example, we considered the 3-D pyramidal quantum dot presented in [13]. It consists of a pyramid InAs quantum dot (pyramid base $d = 12.4$ nm, pyramid

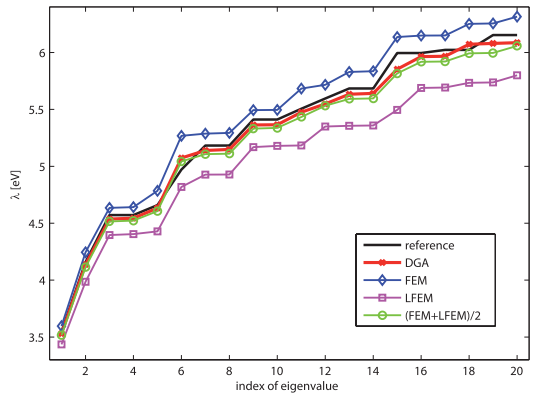

Fig. 2. First 20 eigenvalues on the finest mesh for the cube benchmark.

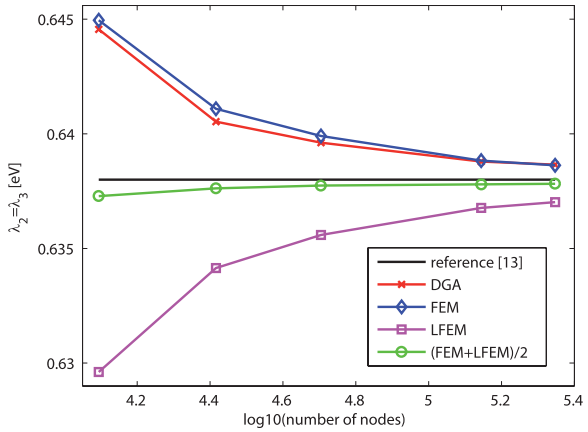

Fig. 3. Convergence with respect to mesh refinement of the second and third eigenvalue $\lambda_2 = \lambda_3$ for the quantum dot benchmark.

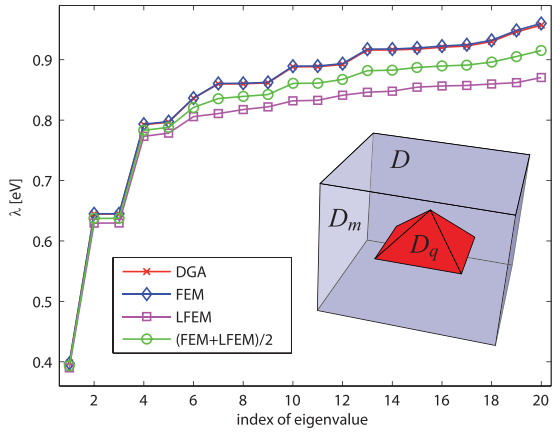

Fig. 4. First 20 eigenvalues on the coarsest mesh for the quantum dot benchmark.

height $h = 6.2$ nm, $q_{\mathrm{InAs}} = 1.5877$) placed in a GaAs matrix ($d_{\mathrm{box}} = 24.8$ nm, $h_{\mathrm{box}} = 18.6$ nm, $q_{\mathrm{GaAs}} = 0.5687$), see Fig. 3. The energy of $u_{\mathrm{InAs}} = 0$ eV is considered in the quantum dot subregion D_q, whereas $u_{\mathrm{GaAs}} = 0.77$ eV is fixed in the surrounding matrix subregion D_m. The obtained results in term of the convergence with respect to mesh refinement of the second and third smaller eigenvalues are compared in Fig. 3 to the ones obtained in [13] with finite differences on a uniform mesh consisting of about 12.5 millions nodes. We note that, in all numerical experiments, $\lambda_I \leq \lambda \leq \lambda_{\mathrm{FE}}$ holds, although this is not true in general [14]. The time required by the eigenvalue solver on the bigger mesh (1 199 652 tetrahedra and 214 965 nodes) has been 1276 s for FEM, whereas it has been about 196 s for both LFEM and DGA. Also in this example DGA exhibits a slightly better accuracy with respect to FEM and LFEM techniques and this behavior holds for all eigenvalues, as Fig. 4 shows for the first 20.

VI. Conclusion

A numerically efficient discrete counterpart of the Schrödinger problem obtained by DGA has been presented. The resulting standard eigenvalue problem is easier and faster to solve with respect to the generalized eigenvalue problem arising from FE. In particular, with DGA there is no need to store the mass matrix, which reduces the memory to maintain the sparse matrices by half. Moreover, there is no need to factorize the mass matrix, with obvious savings in terms of memory and computational time. The numerical results confirm the convenience of DGA with respect to first-order FE both in terms of accuracy and speed. Second-order FE requires a sensible increase of computational effort having at least ten times more unknowns and less sparsity. For this reason, second-order FE starts to be competitive only when the required error tolerance is very small. This is not the case of the applications considered in this paper, where material and geometric parameters are known at most with a few percent accuracy. For this reason, a much smaller tolerance is unjustified in practice.

References

[1] J. Del Alamo, "Nanometre-scale electronics with III-V compound semiconductors," *Nature*, vol. 479, pp. 317–323, Nov. 2011.

[2] D. Breda, D. Esseni, A. Paussa, R. Specogna, F. Trevisan, and R. Vermiglio "Comparison between pseudospectral and discrete geometric methods for modeling quantization effects in nanoscale electron devices," *IEEE Trans. Magn.*, vol. 48, no. 2, pp. 203–206, Feb. 2012.

[3] Q. H. Liu, C. Cheng, and H. Z. Massoud, "The spectral grid method: A novel fast Schrödinger-equation solver for semiconductor nanodevice simulation," *IEEE Trans. CAD*, vol. 23, no. 1, pp. 1200–1208, Feb. 2004.

[4] F. Schwabl, *Quantum Mechanics*. New York, NY, USA: Springer-Verlag, 1992.

[5] R. Specogna and F. Trevisan, "A discrete geometric approach to solving time independent Schrödinger equation," *J. Comput. Phys.*, vol. 230, pp. 1370–1381, Feb. 2011.

[6] E. Tonti, *On the Formal Structure of Physical Theories*. Italy: CNR, 1975.

[7] F. Trevisan and L. Kettunen, "Geometric interpretation of discrete approaches to solving magnetostatic problems," *IEEE Trans. Mag.*, vol. 40, no. 2, pp. 361–365, Mar. 2004.

[8] G. Strang and G. J. Fix, *Analysis of the Finite Element Method*. New York, NY, USA: McGraw-Hill, 1977.

[9] M. Nakamura and M. Hirasawa, "Eigenvalues of the Schröedinger equation by the α-interpolation method," *SIAM J. Appl. Math.*, vol. 43, no. 6, pp. 1286–1293, 1983.

[10] J. Hu, Y.-Q. Huang, and H. Shen, "The lower approximation of eigenvalue by lumped mass finite element method," *J. Comput. Math.*, vol. 22, no. 4, pp. 545–556, 2004.

[11] E. Polizzi, "Density-matrix-based algorithms for solving eigenvalue problems," *Phys. Rev. B*, vol. 79, no. 11, pp. 115112-1–115112-3, 2009.

[12] K. Wu and H. Simon, "Thick-restart Lanczos method for large symmetric eigenvalue problems," *SIAM J. Matrix Anal. Appl.*, vol. 22, no. 2, pp. 602–616, 2001.

[13] T.-M. Hwang, W.-W. Lin, W.-C. Wang, and W. Wang, "Numerical simulation of three dimensional pyramid quantum dot," *J. Comput. Phys.*, vol. 196, no. 1, pp. 208–232, 2004.

[14] M. G. Armentano and R. G. Durán, "Mass-lumping or not mass-lumping for eigenvalue problems," *Numer. Methods Partial Differential Eq.*, vol. 19, no. 5, pp. 653–664, 2003.